# CHEMICAL
# RESEARCH,
# DEVELOPMENT &
# ENGINEERING
# CENTER

CRDEC-TR-005

AD-A203 377

# CONTRIBUTIONS OF PARTICLE ABSORPTION
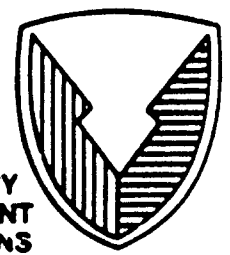# TO MASS EXTINCTION COEFFICIENTS (0.55-14 μm)
# OF SOIL-DERIVED ATMOSPHERIC DUSTS

DTIC
SELECTED
JAN 2 4 1989
D

Hugh R. Carlon
U.S. Army Fellow

RESEARCH DIRECTORATE

December 1988

U.S. ARMY
ARMAMENT
MUNITIONS
CHEMICAL COMMAND

Aberdeen Proving Ground, Maryland    21010-5423

| REPORT DOCUMENTATION PAGE | | Form Approved OMB No. 0704-0188 |
|---|---|---|

| 1a. REPORT SECURITY CLASSIFICATION UNCLASSIFIED | 1b RESTRICTIVE MARKINGS |
|---|---|

| 2a. SECURITY CLASSIFICATION AUTHORITY | 3 DISTRIBUTION/AVAILABILITY OF REPORT |
|---|---|
| 2b. DECLASSIFICATION/DOWNGRADING SCHEDULE | Approved for public release; distribution is unlimited. |

| 4. PERFORMING ORGANIZATION REPORT NUMBER(S) CRDEC-TR-005 | 5. MONITORING ORGANIZATION REPORT NUMBER(S) |
|---|---|

| 6a. NAME OF PERFORMING ORGANIZATION CRDEC | 6b. OFFICE SYMBOL (If applicable) SMCCR-RSP-P | 7a. NAME OF MONITORING ORGANIZATION |
|---|---|---|

| 6c. ADDRESS (City, State, and ZIP Code) Aberdeen Proving Ground, MD 21010-5423 | 7b. ADDRESS (City, State, and ZIP Code) |
|---|---|

| 8a. NAME OF FUNDING/SPONSORING ORGANIZATION CRDEC | 8b. OFFICE SYMBOL (If applicable) SMCCR-RSP-P | 9. PROCUREMENT INSTRUMENT IDENTIFICATION NUMBER |
|---|---|---|

| 8c. ADDRESS (City, State, and ZIP Code) Aberdeen Proving Ground, MD 21010-5423 | 10. SOURCE OF FUNDING NUMBERS | | | |
|---|---|---|---|---|
| | PROGRAM ELEMENT NO. | PROJECT NO. 1L161101 | TASK NO. A91A | WORK UNIT ACCESSION NO. |

11. TITLE (Include Security Classification) Contributions of Particle Absorption to Mass Extinction Coefficients (0.55-14 μm) of Soil-Derived Atmospheric Dusts

12. PERSONAL AUTHOR(S)
Carlton Hugh R., U.S. Army Fellow

| 13a. TYPE OF REPORT Technical | 13b. TIME COVERED FROM 79 Jan TO 82 Dec | 14. DATE OF REPORT (Year, Month, Day) 1988 December | 15. PAGE COUNT 28 |
|---|---|---|---|

16. SUPPLEMENTARY NOTATION

infared

| 17. COSATI CODES | | | 18 SUBJECT TERMS (Continue on reverse if necessary and identify by block number) |
|---|---|---|---|
| FIELD | GROUP | SUB-GROUP | Soils, Optical Extinction, Fort Benning, |
| 20 | 05 | | Dusts, IR Absorption, Atmospheric dusts, |
| | | | Aerosols, Extinction coefficients, Dust minerals. |

19. ABSTRACT (Continue on reverse if necessary and identify by block number)

Mass extinction coefficients of soil-derived atmospheric dusts often are determined largely by the absorption (rather than scattering) by individual particles, especially at longer IR wavelengths. Under many conditions, reasonable estimates of mass extinction coefficients of dusts can be made from absorption coefficients without detailed knowledge of particle optical constants to perform, for example, Mie calculations. This report discusses absorption coefficients of dusts in the visible and IR wavelengths and the physical mechanisms of dust aerosol generation determining that portion of extinction attributable to absorption in a given dust cloud. Some soils, especially clays, can produce dust clouds that are almost pure absorbers at longer IR wavelengths.

infared

| 20. DISTRIBUTION/AVAILABILITY OF ABSTRACT ☒ UNCLASSIFIED/UNLIMITED ☐ SAME AS RPT ☐ DTIC USERS | 21 ABSTRACT SECURITY CLASSIFICATION UNCLASSIFIED |
|---|---|

| 22a. NAME OF RESPONSIBLE INDIVIDUAL SANDRA J. JOHNSON | 22b TELEPHONE (Include Area Code) (301) 671-2914 | 22c OFFICE SYMBOL SMCCR-SPS-T |
|---|---|---|

DD Form 1473, JUN 86        Previous editions are obsolete.

PREFACE

The work described in this report was authorized under Project No.
1L161101A91A, In-House Laboratory Independent Research.  This work was
started in January 1979 and completed in December 1982.

The use of trade names or manufacturers' names in this report does
not constitute an official endorsement of any commercial products.  This
report may not be cited for purposes of advertisement.

Reproduction of this document in whole or in part is prohibited except
with permission of the Commander, U.S. Army Chemical Research, Development and
Engineering Center (CRDEC), ATTN:  SMCCR-SPS-T, Aberdeen Proving Ground, Maryland
21010-5423.  However, the Defense Technical Information Center and the National
Technical Information Service are authorized to reproduce the document for U.S.
Government purposes.

This report has been approved for release to the public.

ACKNOWLEDGMENT

The author acknowledges with sincere appreciation the assistance of
Dennis F. Flanigan, CRDEC, who provided information and illustrations from the
paper he coauthored with H.P. DeLong and which is extensively discussed in
this report.

3

Blank

4

CONTENTS

## LIST OF FIGURES

## LIST OF TABLES

# CONTRIBUTIONS OF PARTICLE ABSORPTION
## TO MASS EXTINCTION COEFFICIENTS (0.55-14 μm)
## OF SOIL-DERIVED ATMOSPHERIC DUSTS

1.        INTRODUCTION


1.1       General.


Optical extinction by atmospheric particulates is a universally known phenomenon but is not as clearly understood for soil-derived dusts as for other classes of aerosols. Calculations can be performed directly for aerosols of spherical particles (e.g., liquid droplets) using the Mie theory,[1] but computational techniques for irregular granules, including most kinds of dust particles, are still being evaluated.[2] This report presents optical data for dusts in the visible and infrared (IR) wavelengths and discusses the physical characteristics of dust aerosols determining that portion of extinction attributable to absorption in a given aerosol or cloud. Localized dust clouds, formed when surface soils are disturbed, are unique among aerosols in that their particle distributions are already determined in situ; and they are largely dependent for their optical behavior upon factors like soil moisture content and mechanisms of dissemination, which determine their airborne particle size distributions.


Extinction coefficients discussed in this report are those used in the Beer-Lambert equation:

$$-\ln T_\lambda = \alpha_\lambda \, CL \tag{1}$$

where

$$\alpha_\lambda = {}^\alpha A_\lambda + {}^\alpha S_\lambda \tag{2}$$

These and subsequent terms are defined in subsection 1.2. Often it is convenient to discuss ratios or relative magnitudes of the coefficients in equation 2. For example, the extinction of strongly absorbing dust particles when their diameters are small compared with the wavelength can be due almost entirely to absorption. That is,

$$\alpha_\lambda \approx {}^{\alpha}A_\lambda$$

where

$${}^{\alpha}S_\lambda \approx 0, \text{ or } {}^{\alpha}_\lambda / {}^{\alpha}A_\lambda \rightarrow 1 \text{ as } {}^{\alpha}S_\lambda \rightarrow 0.$$

Under these conditions, it has been shown[3] that certain simple approximations often are adequate to describe the spectral behavior of aerosol particles, especially in the IR. These approximations work well for dust particles; for example, finely sized talc dusts exhibit an extremely sharp absorption peak at 9.8 $\mu$m and practically no evidence of optical scattering.[4] In this case, a substantial portion of the dust-particle size distribution has small diameters compared to the illumination wavelength [i.e., the size parameter $(\pi D_\mu / \lambda)$ is small, and a Rayleigh-like scattering situation exits]. The measured spectrum of a typical talc dust cloud (7-13.5 $\mu$m) is shown in Figure 1, where the virtual absence of particle scattering is evident toward shorter wavelengths, for example at 7-8 $\mu$m.
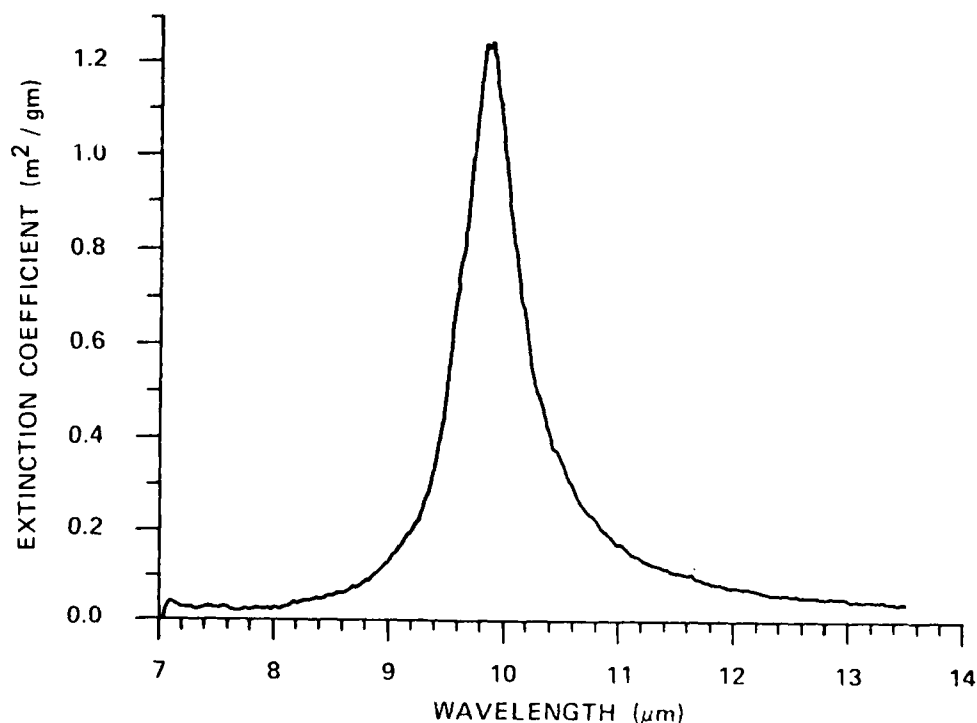


Figure 1. IR Spectrum of a Dust Cloud of Talc (Magnesium Silicate) Particles

Under Rayleigh-like conditions,[3,5]

$$\alpha_\lambda \cdot \rho = {}^\alpha A_\lambda \cdot \rho = {}^k L_\lambda \cdot f(m_\lambda) \tag{3}$$

where $f(m_\lambda)$ is a *function of the complex index of refraction* and is approximately 1.0 for most aerosol particles. Hence, the assumption $f(m_\lambda) = 1.0$ will be used for Rayleigh-region approximations in this report. The reader interested in greater precision should apply the correction for $f(m_\lambda)$ from literature cited number 3.

The imaginary component of the refractive index, $k_\lambda$, is related to the absorption coefficient, ${}^k L_\lambda$ ($\mu m^{-1}$), by the simple expression

$$^k L_\lambda = (4\pi k_\lambda)/\lambda \tag{4}$$

1.2     Definition of Terms.

$\alpha_\lambda$ = optical extinction coefficient at wavelength $\lambda$, $m^2/g$;

${}^\alpha A_\lambda$ = absorption component of the optical extinction coefficient at wavelength $\lambda$, $m^2/g$;

${}^\alpha S_\lambda$ = scattering component of the optical extinction coefficient at wavelength $\lambda$, $m^2/g$;

$C$ = aerosol particle mass concentration, $g/m^3$;

$D_\mu$ = geometric mean aerosol particle diameter, $\mu m$;

$f(m_\lambda)$ = a complex correction factor depending only on $m_\lambda$;[3]

$k_\lambda$ = imaginary part of the complex index of refraction at wavelength $\lambda$, unitless;

${}^k L_\lambda$ = absorption coefficient at wavelength $\lambda$, numerically equal to ${}^\alpha A_\lambda \cdot \rho$ if $f(m_\lambda) = 1.0$ (equation 3), $\mu m^{-1}$;

$L$ = optical path length, m;

$\lambda$ = wavelength, $\mu$m;

$m_\lambda$ or $(n-ik)_\lambda$ = complex index of refraction at wavelength $\lambda$, unitless;

MMD = mass median diameter, $\mu$m;

$n_\lambda$ = real part of the complex index of refraction at wavelength $\lambda$, unitless;

$\rho$ = density of material making up the aerosol particles, g/cm$^3$; and

$T_\lambda$ = optical transmittance at wavelength $\lambda$, unitless.

2.    ATMOSPHERIC ABSORPTION BY SOIL-DERIVED DUSTS

Atmospheric dust extinction data in the literature commonly are reported in units of reciprocal path length (m$^{-1}$, km$^{-1}$, dB/km, etc.). This has the effect of combining $\alpha_\lambda$ and C in equation 1. Such data have limited value because the kinds, mixing ratios, and size distributions of dusts or other aerosols present when the data were taken must be assumed constant if these data are to be used for subsequent predictive purposes in the same geographical areas. It is much more desirable to know the optical (mass) coefficients ($\alpha$s) of the aerosol constituents, so that these data may be universally applied if airborne mass concentrations and particle size distributions can be determined in any real situation. The latter approach is taken in this report.

Optical constants are reported in the literature for many kinds of soils and dusts. Volz published optical constants (2.5-40 $\mu$m) for the dry natural aerosol[6] and for Sahara dust, volcanic pumice, fly ash, and other substances;[7] Pollack et al.[8] reported optical constants (0.2-50 $\mu$m for five naturally occurring rocks: California and Oregon obsidians, basaltic glass, basalt, and andesite; Querry et al.[9] published optical constants

10

(0.2-32.8 µm) for limestone; and Flanigan and DeLong[10] give spectral absorption coefficients (7.7-14 µm) for 70 soil samples gathered from around the world.

In this discussion, atmospheric extinction over the interval 0.55-10.6 µm is considered as a function of typical natural aerosol size distributions.[11] The absorption component of extinction by atmospheric dusts is considered at several laser wavelengths.[11,12] IR absorption spectra (7.7-14 µm) adapted from Flanigan and DeLong's data[10] are discussed with peak values of the absorption coefficient given. Finally, the behavior of an extremely troublesome spectral dust (Georgia red clay) is examined. The complex refractive indices of several aerosol materials are shown in Table 1, with absorption coefficients calculated using equations 3 and 4 for the approximation $f(m_\lambda) = 1.0$ in Rayleigh region (only).[11,12]

Note that the condition $D_\mu \ll \lambda$ must exit if absorption coefficients are to be accurately approximated by equations 3 and 4.[13] For example, concern was expressed[13] regarding the method used to obtain the values of Schleusener,[12] which are listed in Table 1 (also, see the first note in Table 1).

Patterson[11] has shown that the overall extinction expected for natural soil-derived atmospheric aerosol should be approximately neutral (i.e., wave-length independent) over the 0.55-10.6 µm spectral range. Furthermore, this wavelength independence does not appear to change with increasing or decreasing visibility (i.e., the aerosol mass concentration). This result is expected whether or not aerosols are of local origin and is not strongly dependent upon values assumed for $k_\lambda$. Typical measured aerosol size distributions upon which these findings are based are shown in Figure 2.[11] The solid line represents a distribution measured under conditions of greatly reduced visibility (≈ 8 km), whereas the dashed line represents a size distribution of much lower total mass concentration measured under conditions of only slightly reduced visibility. The mode between 1 and 10 µm appears in both distributions, whereas the other modes are seen only in one distribution or the other (see article by Patterson[11] for details). A relatively heavy natural dust-aerosol mass concentration is considered to be 0.002 g/m³, whereas a concentration for only slightly reduced

11

visibility would be ~0.0001 g/m$^3$. Much higher concentrations occur, of course, in dust clouds raised in the immediate vicinity of distrubed soil surfaces.

Table 1.  Optical Constants of Several Atmospheric Aerosol Materials

| Material | $\lambda$ | $n_\lambda$ | $k_\lambda$ | $\alpha A_\lambda \cdot \rho = k_{L_\lambda}$ | $\alpha A_\lambda$ | Note | Literature cited | Assumed |
|---|---|---|---|---|---|---|---|---|
| Natural aerosol | 0.55 | 1.525 | 0.005 | (0.114) | (0.048) | 1 | 11 | $\rho$ = 2.4 |
| Natural aerosol | 0.63 | 1.525 | 0.005 | (0.1) | (0.042) | 1 | 11 | $\rho$ = 2.4 |
| Natural aerosol | 0.9 | 1.65 | 0.005 | (0.07) | (0.029) | 1 | 11 | $\rho$ = 2.4 |
| Natural aerosol | 1.06 | 1.65 | 0.005 | (0.059) | (0.025) | 1 | 11 | $\rho$ = 2.4 |
| Natural aerosol | 3.5 | 1.66 | 0.016 | 0.057 | 0.024 | 2 | 11 | $\rho$ = 2.4 |
| Natural aerosol | 5.0 | 1.59 | 0.032 | 0.08 | 0.034 | 2 | 11 | $\rho$ = 2.4 |
| Natural aerosol | 10.6 | 1.7 | 0.07 | 0.083 | 0.035 | 2 | 11 | $\rho$ = 2.4 |
| Natural aerosol | | 1.87 | 0.3 | 0.356 | 0.148 | 2 | 11 | $\rho$ = 2.4 |
| Natural aerosol | 1.06 | | 0.036 | (0.427) | (0.18) | 1 | 12 | $\rho$ = 2.4 |
| Natural aerosol | 9.6 | | 0.29 | 0.38 | 0.16 | 2 | 12 | $\rho$ = 2.4 |
| Natural aerosol | 10.6 | | 0.135 | 0.16 | 0.07 | 2 | 12 | $\rho$ = 2.4 |
| Quartz | 1.06 | | negligible | | | - | 12 | $\rho$ = 2.4 |
| Quartz | 9.6 | | 0.325 | 0.425 | 0.16 | 2 | 12 | $\rho$ = 2.66 |
| Quartz | 10.6 | | 0.051 | 0.06 | 0.02 | 2 | 12 | $\rho$ = 2.66 |
| Acetylene soot | 1.06 | | 0.586 | 6.95 | 4.09 | 3 | 12 | $\rho$ = 1.7 |
| Acetylene soot | 9.6 | | 0.733 | 0.96 | 0.56 | 2 | 12 | $\rho$ = 1.7 |
| Acetylene soot | 10.6 | | 0.732 | 0.87 | 0.51 | 2 | 12 | $\rho$ = 1.7 |

NOTES:

1. For the Mie and geometric scattering cases, the interrelationships between $k_\lambda$ and $\alpha A_\lambda$ are more complex,[13] and other techniques for the approximation of extinction coefficients apply.[3] The values shown in parentheses are calculated using equations 3 and 4 but would be approximately correct only for fine natural aerosol particles.

2. Calculated from equations 3 and 4 for the Rayleigh case ($D_\mu \ll \lambda$).

3. Probably a good approximation even at $\lambda$ = 1.06 μm because soot typically is composed of particles with diameters predominantly near $D_\mu$ = 0.1 μm, and the Rayleigh case ($D_\mu \ll \lambda$) applies.
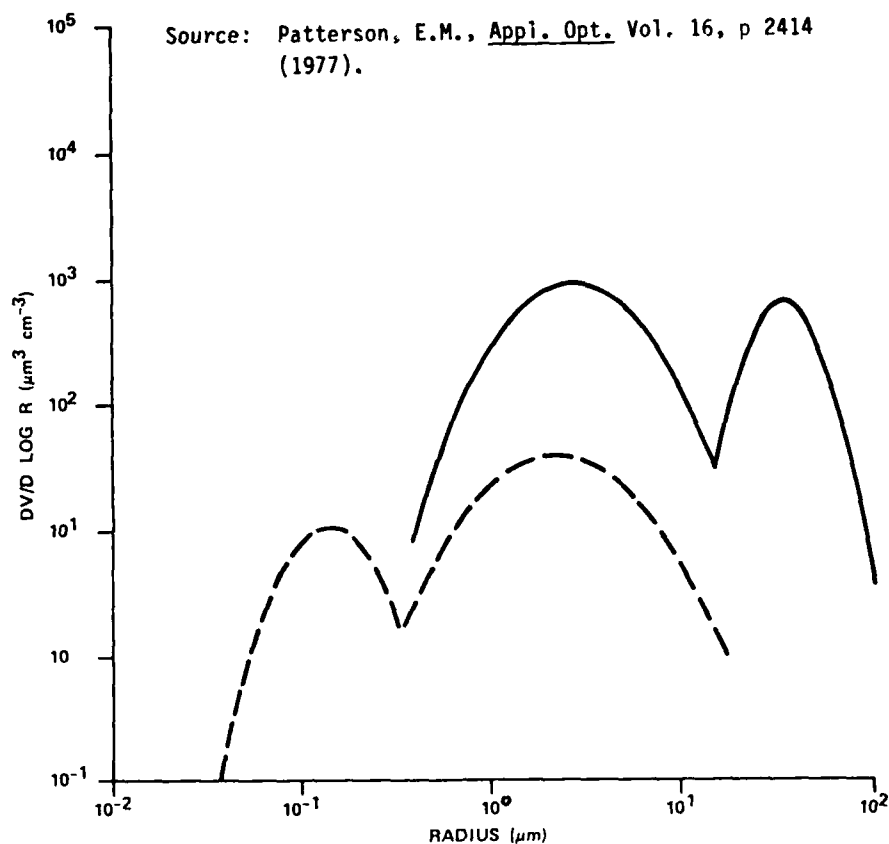
Figure 2. Typical Measured Aerosol Size Distributions

3.      DUST ABSORPTION IN THE 7.7-14 μm SPECTRAL REGION

Neutral attenuation with wavelength may be a generally valid assumption over long atmospheric paths that integrate spectral features due to various natural aerosols, but dense localized soil-derived dust clouds can have pronounced spectral character under some conditions. This is especially true at longer IR wavelengths in the 7-14 μm atmospheric window region where, because of particle size distributions found in some localized dusts, a significant portion of the total optical extinction can arise from absorption of the particles rather than from optical scattering. Thus, dusts with large absorption coefficient (large imaginary indices) in this wavelength region and with relatively small particle sizes can behave as pure absorbers. Talc was mentioned as an example (Figure 1) where $\alpha\lambda/^{\alpha}A_\lambda \approx 1.0$, but the author's measurements indicate that for most dusts this ratio varies between 2 and 4. That is, most localized dust clouds

13

derive from one-fourth to one-half of their extinction from particle absorption in the 7-14 μm IR window region.

It is very important to appreciate the distinction between particle size distributions found in surface soils and distributions found in airborne dust clouds generated from these surface soils. It is true that soil, containing a large fraction of small particles or "fines," when disturbed tends to produce a cloud or more finely sized dust particles than will a coarse soil.[14] The ultimate extension of this is the natural aerosol (for example, the dashed curve in Figure 2), whose particles tend to be so fine that they are relatively unaffected by settling due to gravity and can remain airborne for long periods of time.

Nearly all soils, and especially clays,[15] contain small fractions of particles with diameters of a few micrometers or less that, once airborne, settle at velocities <1 mm/s. Clouds of such fine particles can, therefore, persist for long periods in the slightest atmospheric turbulence. They usually are dispersed by air currents long before their particles resettle to the soil surface. Examples of differences in dust-particle size distributions between dust clouds and the soils producing them are discussed later.

Dusts with extremely fine particles and strong absorption bands can contribute to spectral (i.e., wavelength-dependent) behavior of the extinction coefficient, since $\alpha_\lambda$ is the summation (equation 2) of the optical scattering component, which is reduced at a given wavelength as the mean size of the particle distribution shifts to values smaller than $\lambda$. The absorption component can then become significant or even predominant in determining the overall value of $\alpha_\lambda$. For example, it was learned in an earlier program[16] that the finest-sized, most troublesome spectral dusts in the field environment were those rising from dry dirt roads traveled heavily by rubber-tired vehicles that continually gristed soil particles on the road surfaces. Other workers[17] found that 250 passes by a light vehicle over fine-grained soils produced an increase from 4 to 14% in the fraction of surface particles <74 μm (a standard test procedure for dusts involves determination of the fraction passing through a 74 μm mesh screen or sieve). Helicopters can raise troublesome dust clouds even from coarse soil surfaces because of their strong downward propeller wash, momentarily lifting

14

particles >200 μm into the air.  These data[17] are based on soil samples
containing 0.2-2.0% moisture.  Because many soils consist of agglomerates
of very fine particles, vehicular gristing action at the surface under dry
conditions that discourages reagglomeration ensures that any disturbance of
the surface will produce clouds of very fine particles that are almost like
haze in their drift characteristics.  Furthermore, larger particles raised
from the surface tend to settle from the cloud much more rapidly than the
fines.  A drifting cloud of absorbing dust reaches maximum absorption-to-
scatter ratio due to the loss of larger predominantly scattering particles
on the one hand and dispersion or diminution of concentration (C) of the
cloud on the other.  In the 7-14 μm atmospheric window region, for example,
road dusts in Georgia and Utah were capable of producing extinction spectra
with peak absorptions 40-50% greater than the band shoulders.[16]

On first consideration, it would seem logical that explosives would
be an effective way to quickly disseminate large quantities of fine dust,
but tests have shown that this is not the case.  Buried or ground-impacted
explosives throw large quantities of soil into the air, but most of the
disturbed subsurface soil is heavily agglomerated because it is not subjected
to the drying and gristing effects common to surface activity.  Short-lived
clouds of large mean particle size are produced by explosives.  These tend
to extinguish visible or IR radiation in a broadband or neutral manner simply
by blocking or scattering it.  The traditional dust of battle, although
sometimes locally troublesome, has rarely ended a military operation by
reason of prolonged visibility reduction.

Other work has been done to characterize the physical properties of
the dust environment in the vicinity; for example, of military activities.[17]
Table 2 shows that topsoil taken from the upper 6-7 mm of the earth's surface
usually has a mass median diameter (MMD) considerably smaller than that of
subsurface soil.  Thus, topsoil usually contains a greater percentage of subsieve
(<74 μm) particles than subsurface soil contains.  The added gristing action
of surface activity cannot be judged from Table 2 because details of sample sites
and conditions are not given, but we see that even extremely fine materials
such as Alaskan river-bottom silt, when dried, still have typical MMDs as large
as 32 μm.  Thus, the lower tail of the particle size distribution for this

15

sample would contain a large fraction of particles having diameters comparable with those of visible and IR wavelengths that could be raised from a dried soil sample to produce a dust cloud of very fine particles.

Table 2.  Dust Content of Typical United States Soils[17]

| Location | Description | MMD (μm) | Percent Dμ < 74 μm |
|----------|-------------|----------|--------------------|
| Perryman, MD | Test course topsoil | 330 | 17.4 |
| | Test course subsoil | 326 | 8.2 |
| Dugway, UT | Proving Ground topsoil | 254 | 12.3 |
| | Proving Ground 3 in. subsoil | 326 | 8.6 |
| Kenvil, NJ | Topsoil | 480 | 24.0 |
| | Subsoil | 105 | 42.0 |
| Redstone, AL | Arsenal topsoil | 290 | 17.0 |
| | Arsenal subsoil | 685 | 4.0 |
| White Sands, NM | Missile range 2 in. topsoil | 220 | 3.0 |
| | Missile range 6 in. subsoil | 228 | 5.0 |
| San Antonio, TX | Black Gumbo topsoil | 840 | 2.7 |
| | Black Gumbo 3 in. subsoil | 840 | 1.4 |
| | Clay topsoil | 238 | 17.6 |
| | Clay 3 in. subsoil | 665 | 14.0 |
| | Sandy loam topsoil | 122 | 17.7 |
| | Sandy loam 3 in. subsoil | 157 | 7.1 |
| Delta. AK | Delta river bottom silt | 32 | 83.6 |
| | Delta river bottom surface | 460 | 2.3 |
| | Delta river bottom 3 in. subsurface | 340 | 1.2 |

Table 3 shows data[17] for caliche (very fine young limestone) from Fort Hood, WA, and dusts from Yuma Proving Ground, AZ, which were about 40% quartz. The remaining 60% consisted of clay, carbonates, and gypsum.  Nearly 10% of the particles in these soil samples lay in the 0-5 μm particle size

16

range, and they would produce strong absorption bands in the 7-14 μm IR wavelength region if raised into the air as dust clouds.

Table 3. Particle Size Distribution in Soil Below 74 μm[17]

|  | Yuma | |
| Size (μm) | Proving Ground | Fort Hood |
| --- | --- | --- |
| 0-5 | 9 | 9 |
| 5-10 | 15 | 13 |
| 10-20 | 22 | 28 |
| 20-40 | 34 | 31 |
| 40-74 | 18 | 18 |

The most extensive treatment of absorption by dust in the 7.7-14 μm wavelength region is that of Flanigan and DeLong, U.S. Army Chemical Research, Development and Engineering Center (CRDEC).[10] They found that 70 soil samples taken from locations around the world could be characterized as combinations of the five basic soil-derived constituents shown in Table 4 where their peak IR absorption locations are shown in wave numbers and in wavelength.

Table 4. Peak Positions of the IR Bands of the Common Dust Minerals[10]

| Kaolinite | | Illite | | Montmorillonite | | Silica | | Calcium carbonate | |
| $cm^{-1}$ | μm | $cm^{-1}$ | μm | $cm^{-1}$ | μm | $cm^{-1}$ | μm | $cm^{-1}$ | μm |
| --- | --- | --- | --- | --- | --- | --- | --- | --- | --- |
| 700 | 14.29M | 913 | 10.95M | 913 | 12.75M | 780 | 12.67M | 714 | 14.0W |
| 755 | 13.25W | 1031 | 9.7VS | 1040 | 9.6VS | 800 | 12.50W | 845 | 11.83W |
| 790 | 12.66W | 1117 | 8.95M* | 1117 | 9.95M* | 1090 | 9.17VS | 873 | 11.45S |
| 913 | 10.95S | | | | | 1175 | 8.51S* | 1430 | 6.85VS** |
| 938 | 10.66M | | | | | | | | |
| 1010 | 9.90VS | | | | | | | | |
| 1035 | 9.66VS | | | | | KEY: W = weak | | | |
| 1100 | 9.09S | | | | | M = moderate | | | |
| 1115 | 8.97S | | | | | S = strong | | | |
| | | | | | | VS = very strong | | | |

*Shoulder.
**Extends well into the 700-1,300 $cm^{-1}$ region.

17

The compositions of the samples are shown in Table 5, and the IR spectra of these samples are shown in Figure 3.

Table 5.  Relative Concentrations of the Common Dust Minerals in Soil Samples[10]

| Sample No. | Location | Kaolinite | Illite, Mont- morillonite | Silica | Calcium carbo- nate |
|---|---|---|---|---|---|
| 3 | Baroufoss, Norway | | High | High | |
| 4 | Fairbanks, Alaska | Trace | High | High | |
| 7 | Edmonton, Canada | Trace | High | High | |
| 10 | Port Angelos, Washington | Trace | High | High | |
| 13 | Longview, Washington | | High | High | |
| 15 | St. Paul, Minnesota | | High | High | |
| 26 | Detroit, Michigan | | High | High | |
| 27 | Logan, Utah | | High | Low | Low |
| 34 | Columbus, Ohio | Trace | High | High | |
| 37 | Derby, Colorado | Low | Medium | High | |
| 40 | Manhattan, Kansas | Trace | High | High | |
| 45 | Tokyo, Japan | Trace | High | High | |
| 47 | Los Angeles, California | Low | High | High | |
| 48 | Atlanta, Georgia | High | | Low | |
| 50 | Tucson, Arizona | Trace | High | Medium | Trace |
| 55 | Oahu, Hawaii | High | | Low | |
| 56 | Manila, Phillipines | | High | High | |
| 57 | Panama Canal Zone | Medium | Medium | High | |
| 58 | Leedon Park, Singapore | High | | Low | |
| 60 | Maguga, Kenya | High | | Low | |
| 61 | Katherine, Australia | High | | Medium | |
| 64 | Durban, South Africa | High | | Low | |

The samples were carefully prepared before being pressed into KBr pellets.  The spectra of the dust pellets and of fine airborne samples of the same dusts agreed, leading the authors to conclude that (especially at these longer wavelengths) particle size and scattering do not significantly affect the results.  The authors were aware of particle diameter effects, related to those discussed by Jennings et al.,[13] on their measurements.  They estimated that their peak absorption coefficients might be from 10 to 30% larger than measured because of these effects.  The spectra in Figure 3 were normalized by dividing the value of $^{\alpha}A_{\lambda}$ at each wavelength by the peak value of the strongest band,
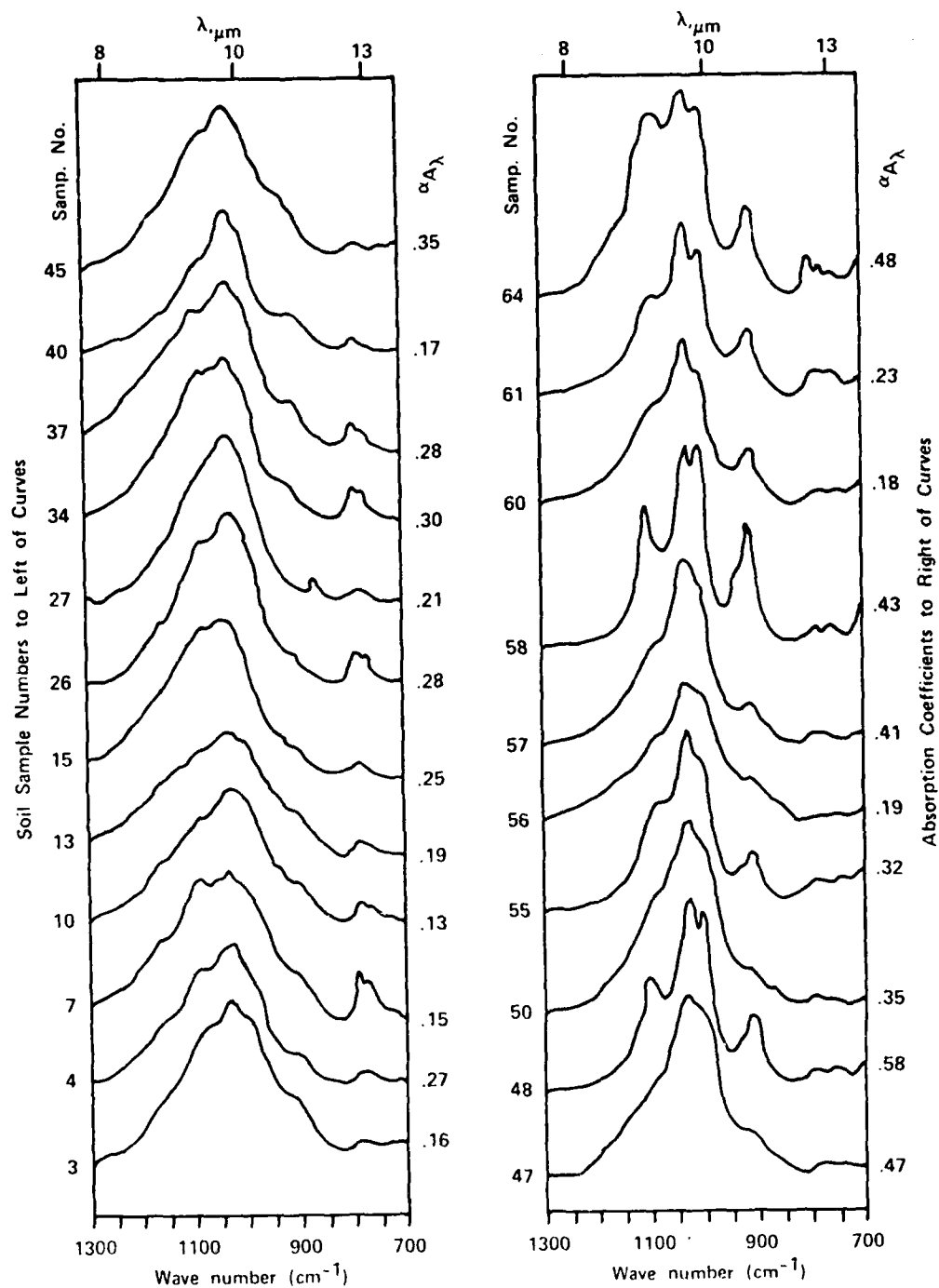
Source: Flanigan, D.F., and DeLong, H.P., _Appl. Opt._ Vol. 10, p 51 (1971).

Figure 3. Spectra of Selected Soil Samples

and the units were converted by the author to those conventional in aerosol spectroscopy (equations 1 and 2); namely, square meters per gram. The soil sample number is shown to the left of each spectrum, and the absorption coefficient of the strongest peak is shown to the right end of each spectrum. Values of $^\alpha A_\lambda$ can be converted directly to $^k L_\lambda$ values using equation 3 if the density $\rho$ of the particles is known and if the assumptions apply. In that case, $k_\lambda$ can be obtained from equation 4.

To find the value of $^\alpha A_\lambda$ for any spectrum or wavelength, proceed as follows. The bottom spectra (sample on left-hand side of the figure and sample 47 on right-hand side) are drawn to correct scale with the base lines (labeled in wave numbers). The peak absorption values ($0.16$ $m^2$/g and $0.47$ $m^2$/g, respectively) are shown to the right of each spectrum. Place a ruler vertically on either bottom spectrum and measure the distance from the base line to the highest absorption peak. This distance is a constant for all curves. Thus, the reader can move from one spectrum to another, measure this constant distance down from the highest absorption peak for each curve, and construct a horizontal base line for each curve at that point. The peak value of $^\alpha A_\lambda$ shown to the right of each curve is then used to graduate the ordinate of each spectrum from its base line.

The kaolinite soils are particularly strong absorbers in the 9.6-9.9μm wavelength region and are often found in finely divided surface clays capable of producing clouds of haze-like dust and of intense spectral activity in this wavelength region. For example, wheeled vehicles on dry, heavily traveled, dirt roads of kaolinite-rich Georgia red clay produce dust clouds among the most IR-absorptive of any found. In such dusts, it is not uncommon for large fractions of collected airborne samples to have submicrometer particle diameters.

Field tests were conducted near Columbus, GA, during development by CRDEC of an IR system described by Ballard et al.[16] The red soil there contained large deposits of kaolinite (aluminum silicate); and an analysis of surface soil from the test site (a dirt road) showed that it contained 65% silica, 17% silicates (predominantly kaolinite), and 18% other substances. When dust clouds were raised by the movement of vehicles along the road, an analysis of the collected dust showed that it contained 20% silica,

33% silicates (predominantly kaolinate), and 47% other substances. Thus, these analyses showed that the dust clouds contained much higher percentages of fine kaolinite particles than did the surface soil that produced them. Silica (sand), the major constituent of the surface soil, usually is found in comparatively large granules that quickly settle back to the surface when disturbed. Thus, an automatic size separation takes place during dust-cloud generation.

Particle size distributions also were determined (using cascaded impactors) for the natural background aerosol and for the kaolinite-rich dust clouds; these are shown in Figure 4.



PARTICLE SIZE DISTRIBUTION        CHEMICAL AND PHYSICAL
                                          PROPERTIES

CHEMICAL COMPOSITION OF DUST:

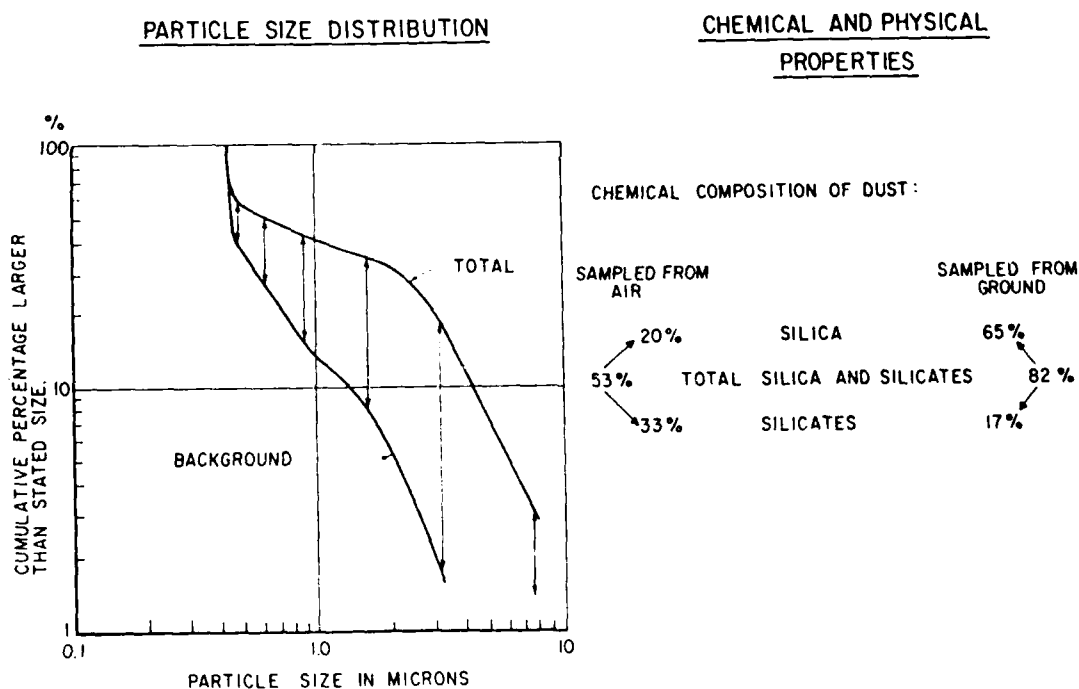| | SAMPLED FROM AIR | | SAMPLED FROM GROUND |
|---|---|---|---|
| | 20% | SILICA | 65% |
| | 53% | TOTAL SILICA AND SILICATES | 82% |
| | 33% | SILICATES | 17% |

Figure 4. Cumulative Particle Size Distributions Measured
for Dust Clouds of Georgia Red Clay

Both curves are from field tests conducted near columbus, GA.  The
local background aerosol (lower curve, labeled BACKGROUND) was very fine,
with only ~2% of the particles >3 μm in diameter.  By comparison, an
average dust cloud (upper curve, labeled TOTAL) contained nearly 20% of
particles >3 μm diameter but only  ~2% > 9.8 μm, which is the diameter
corresponding to the wavelength at which peak IR dust extinction coefficients
were measured in these tests.  The Mie size parameter[1,3] $\pi \cdot D_\mu / \lambda$
for $\lambda$ = 9.8 μm is 0.32 $D_\mu$.  From the upper curve of Figure 4, the
median diameter of particles in these dust clouds was 1-2 μm, corresponding
to a size parameter of 0.32-0.64.  For a 9.8 μm observation wavelength,
this approaches a Rayleigh-like scattering situation with $D_\mu \ll \lambda$, and
we would expect the cloud absorption to make a significant contribution to
total IR extinction.  That this actually did happpen is indicated by the
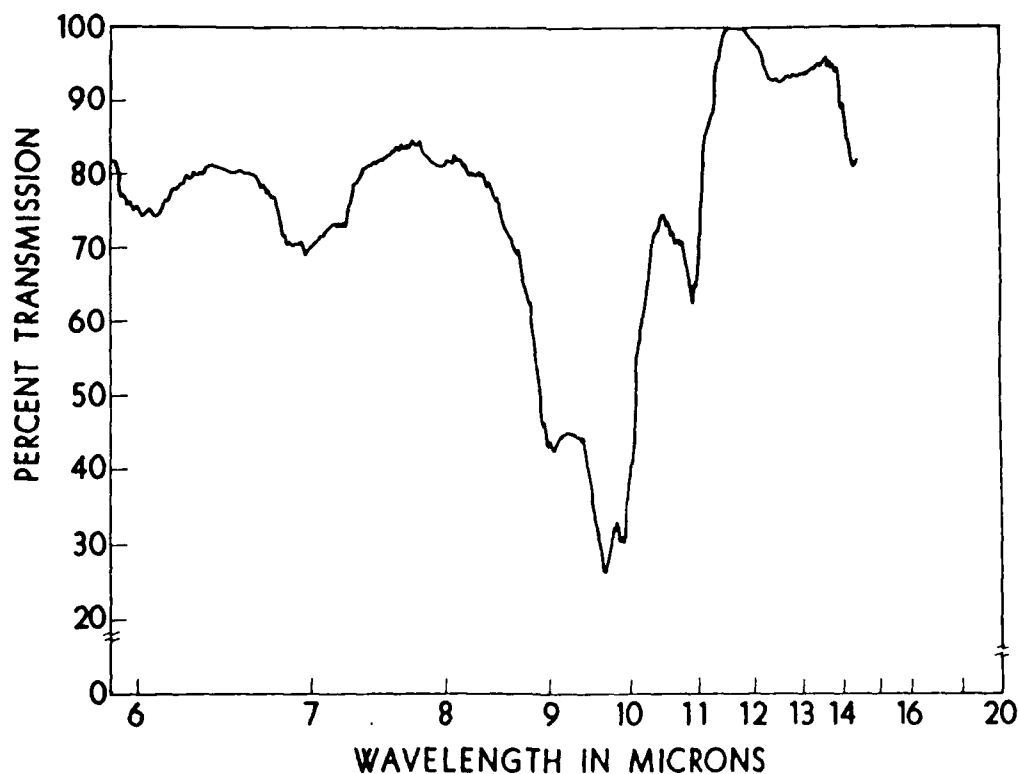spectrum of one of the test dust clouds, shown in Figure 5.



Figure 5.   IR Spectrum of a Dust Cloud of Georgia Red Clay

For comparison purposes, the peak absorption coefficient of the
band at 9.8 µm, from sample 48 in Figure 3 for Georgia kaolinite, is
$^{\alpha}A_{9.8} = 0.58\ m^2/g$. The similarity of these spectra is readily apparent,
except that Christiansen-like effects[18] apparently occur in the spectrum of the
dust in air (Figure 5) near 7.4 and 12 µm, which do not occur in the spectrum
of the dust in KBr (Figure 3). Reduced transmission toward shorter wavelengths
shown in Figure 5 is probably due to scattering by larger dust particles in
the cloud. During the field trials, a filter transmissometer[16] continually
monitored the band at 9.8 µm in Figure 5 (spectral halfwidth ~1.0 µm,
attributed to kaolinite absorption) and ratioed it to the total extinction
across all wavelengths in the 7-14 µm atmospheric window to determine the
percentage of total signal extinction in this window that was due to absorption
only.

The results are shown in Figure 6, where the arrows represent the
time history of data as a red clay dust cloud entered the IR beam and dispersed
over a total period of ~25 s. The kaolinite absorption band at 9.8 µm
accounted for a maximum of ~20% of the signal extinction (abscissa) when
the total extinction was ~60% [(i.e., when the signal transmission was 40%
(ordinate)]. In other words, the 9.8 µm kaolinite dust band, by absorption
only, accounted for about one-third of the total extinction by the dust cloud
over the entire 7-14 µm window region, with the remainder of the extinction
being contributed by absorption at wavelengths other than 9.8 µm, and
optical scattering of airborne particles. The particle size distribution is
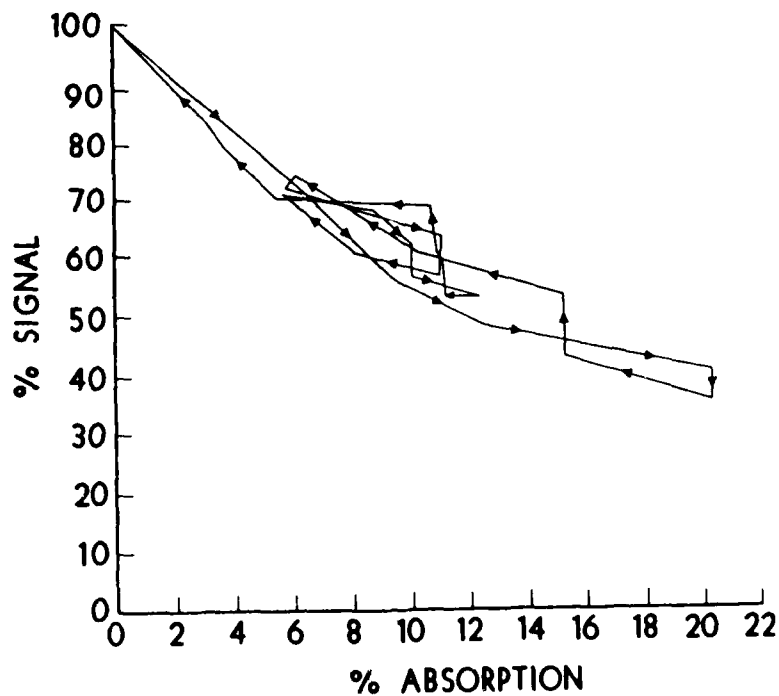shown in Figure 4 (uppercurve).

Figure 6.   Extinction of IR Radiation in the 7-14 μm Window Region
by a Dust Cloud of Georgia Red Clay


The time history of another cloud is shown directly in Figure 7,
where the percentages of total signal, S (top curves), and absorption, A
(lower curve), are plotted as functions of time.  This cloud produced 24%
absorption by the 9.8 μm band when the total signal extinction by absorp-
tion and scattering in the 7-14 μm window region exceeded 60%; that is,
transmission was ~30%.  Thus the 9.8 μm absorption band accounted for
more than one-third of the total 7-14 μm extinction in this case.
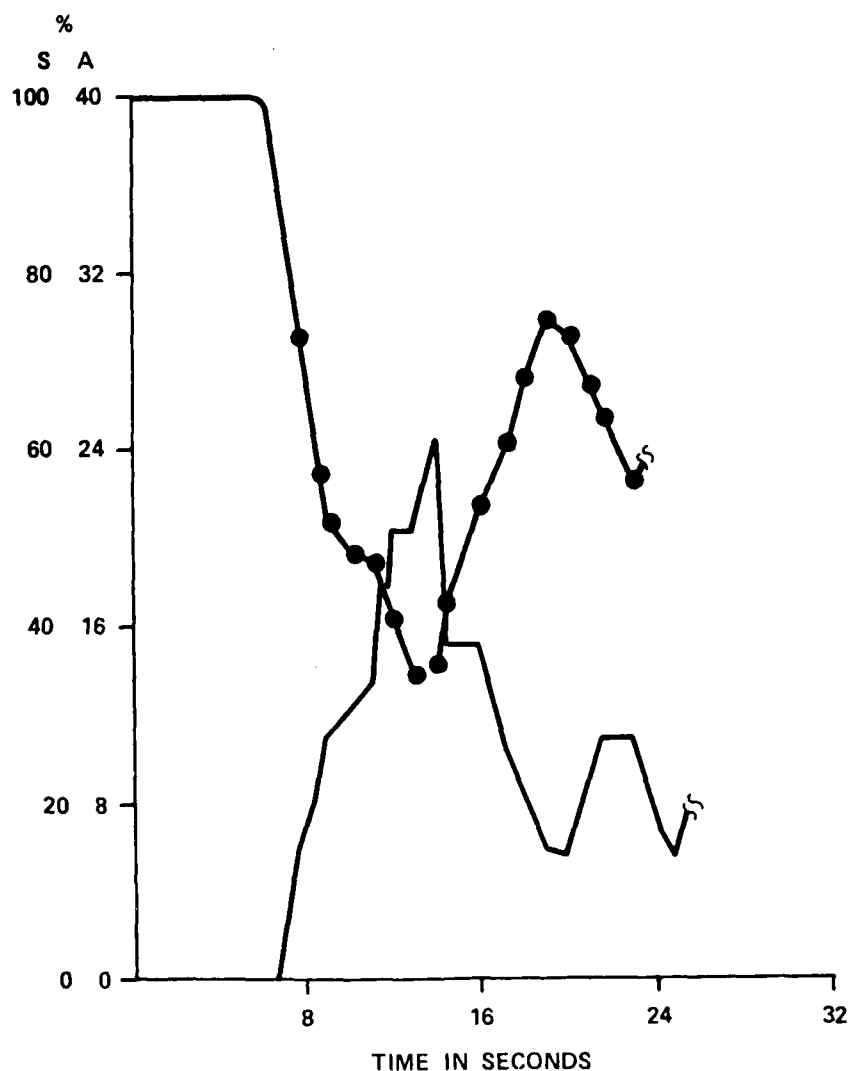
Figure 7.   Time History of IR Extinction in the 7-14 μm Window Region
            by a Dust Cloud of Georgia Red Clay

4.      CONCLUSIONS

        Optical constants and mass absorption coefficients of many soil-derived
dusts are presented, and approximation techniques were discussed that are applicable
when dust-particle size is small compared with wavelength, that is, in the Rayleigh
scattering regime.  It has been shown using experimental spectra for airborne dust
clouds that the particle absorption contribution to the mass extinction coefficient
is especially significant at longer IR wavelengths; for example, in the 7-14 μm

25

atmospheric window, where this contribution can range from ~25 to 50%, for localized field concentrations of dusts from soils like Georgia red clay, to nearly 100% for prepared finely sized minerals like talc. The mechanisms determining the optical properties of dust clouds raised from disturbed soil surfaces are complex and not obvious. The more important mechanisms have been considered here.

## LITERATURE CITED

1. Mie, G., Ann. Phys. (Leipzig) Vol. 25, p 377 (1908).

2. Acquista, C., "Validity of Modifying Mie Theory to Describe Scattering Nonspherical Particles," Appl. Opt. Vol. 17, p 3851 (1978).

3. Carlon, H.R., "Practical Upper Limits of the Optical Extinction Coefficients of Aerosols," Appl. Opt. Vol. 18, pp 1372-1375 (1979).

4. Carlon, H.R., "Durable Narrow Absorption Band Infrared Filters Utilizing Powdered Mineral Materials on Polyethylene Substrates," Appl. Opt. Vol. 1, pp 603-605 (1962).

5. Carlon, H.R., Anderson, D.H., Milham, M.E., Tarnove, T.L., Frickel, R.H., and Sindoni, O.I., "Infrared Extinction Spectra of Some Common Liquid Aerosols," Appl. Opt. Vol. 16, pp 1598-1605 (1977).

6. Volz, F.E., "Infrared Refractive Index of Atmospheric Aerosol Substances," Appl. Opt. Vol. 11, p 755 (1972).

7. Volz, F.E., "Infrared Optical Constants of Ammonium Sulfate, Sahara Dust, Volcanic Pumice, and Fly Ash," Appl. Opt. Vol. 12, p 564 (1973).

8. Pollack, J.B., Toon, O.B., and Khare, B.N., Icarus Vol. 19, p 372 (1973).

9. Querry, M.R., Osborne, G., Lies, K., Jordan, R., and Coveney, R. M., Jr., "Complex Refractive Index of Limestone in the Visible and Infrared," Appl. Opt. Vol. 17, p 353 (1978).

10. Flanigan, D.F., and DeLong, H.P., "Spectral Absorption Characteristics of the Major Components of Dust Clouds," Appl. Opt. Vol. 10, p 51 (1971).

11. Patterson, E.M., "Atmospheric Extinction Between 0.55 μm and 10.6 μm Due to Soil-Derived Aerosols," Appl. Opt. Vol. 16, p 2414 (1977).

12. Schleusener, S.A., Lindberg, J.D., White, K.O., and Johnson, R. L., "Spectrophone Measurements of Infrared Laser Absorption by Energy, Atmospheric Dust," Appl. Opt. Vol. 15, p 2546 (1976).

13. Jennings, S.G., Pinnick, R.P., and Gillespie, J.B., "Relation Between Absorption Coefficient and Imaginary Index of Atmospheric Aerosol Constituents," Appl. Opt. Vol. 18, p 1368 (1979).

14. Gillette, D.A., and Walker, T.R., Soil Sci. Vol. 123, p 97 (1977).

15. Millot, G., Sci. Am. Vol. 240, No. 4, p 109 (1979).

16. Ballard, S.S., and Wolfe, W.L., "Recent Developments in Infrared Technology," Appl. Opt. Vol. 1, p 547 (1962); see "Lopair," p 551.

17.  Engelhardt, R.E., and Knebel, G.W., Characteristics of the Dust Environment in the Vicinity of Military Activities, Report AR-642, U.S. Army Mobility Equipment Research and Development Center, Fort Belvoir, VA, January 1968, UNCLASSIFIED Report.  (AD 665 439)

18.  Carlon, H.R., "Chritiansen Effect in IR Spectra of Soil-Derived Atmospheric Dusts," Appl. Opt. Vol. 18, p 3610 (1979).